Detecting Thermal Discomfort of Drivers Using Physiological Sensors and Thermal Imaging

Mohamed Abouelenien
University of Michigan-Dearborn

Mihai Burzo
University of Michigan-Flint

***Abstract*—Recent technological developments have been used extensively in manufacturing vehicles in order to improve the driving experience and add multiple safety features. This article introduces a novel machine learning approach using physiological sensors and thermal imaging of the subjects to detect human thermal discomfort in order to develop a fully automated climate control system in the vehicles that does not need any explicit input from individuals. To achieve this goal, a dataset of thermal videos and physiological signals from 50 subjects is collected, an extensive analysis of different feature sets is conducted, a multimodal approach is experimented, and a cascaded classification system is proposed. Our results evidently show the capability of specific feature sets of detecting human thermal discomfort as well as the superior performance of integrating multimodal features.**

According to the In-Car Study run by Arbitron, drivers stay in vehicles for approximately 20 h every week.[1] Hence, a real-time system that automatically senses the state of thermal discomfort of the vehicle's occupants can assist in creating better environmental conditions inside a vehicle. Moreover, research studies indicated that increasing the temperature in a vehicle by four degrees Celsius can potentially save 22% of the compressor power, which can

Digital Object Identifier 10.1109/MIS.2019.2938713
Date of publication 30 August 2019; date of current version 18 November 2019.

approximately increase the coefficient of performance by 13%. More importantly, a driver with a thermally comfortable sensation will be less stressed, less fatigued, and more alert, which results in safer driving conditions for the vehicle's occupants as well as for pedestrians.

Currently, the traditional and most widely used mean of controlling the parameters of a vehicle's environment is through a static environmental condition control, which maintains the driver's space in a certain thermal state. Instead, a system that is aware of the real-time thermal sensation of a vehicle's driver can provide an effective assessment of the thermal conditions and, thus, results in an increased comfort level while improving fuel economy.

Measuring the thermal sensation levels of subjects can be achieved via thermal imaging and physiological signals. Thermal imaging is a noninvasive means of capturing thermal measurements from the heat-emitting sources for a wide variety of applications. Physiological signals provide rich information on the individual's health status and responses to different stimuli. With the continuous advancements in the sensors technology, automotive companies started developing seats and seat belts that are capable of measuring specific physiological measurements in order to detect driver's drowsiness, such as the heart and respiration rates. In our previous work, we showed that the multimodal modeling of the human behavior achieves superior performance compared to using a single modality.[2,3] We also showed the feasibility of detecting thermal discomfort using physiological signals.[4]

In this article, we propose a system that is composed of a low-end thermal camera and sensor-based setup that can be installed in the steering wheels in vehicles. In particular, the article provides four main contributions. First, a dataset of sensorial measurements and thermal videos of 50 human subjects is collected using an insulating enclosure attached to an air conditioning and heat pump unit to simulate the conditions in vehicles. Second, we perform an extensive analysis of the different types of signals that are collected in order to determine the features that are most capable of indicating the subjects' thermal sensation. Third, we propose a multimodal learning approach that integrates features from the thermal and physiological modalities to enrich the extracted features for the learning process. Finally, we introduce a cascaded classification system that applies a cascade of classifiers to automatically and reliably detect human thermal discomfort.

RELATED WORK

Wearable sensors have been widely used in order to detect different human activities[5] and human comfort levels.[6] Over the past years, extensive research has been conducted in order to develop intelligent and autonomous vehicles that can provide assistance for more comfortable and safer driving.[7–9]

Research studies have been conducted to detect thermal comfort levels in indoor environments.[10] For instance, a nonlinear regression model was proposed to control thermal discomfort indoors using the PMV model.[11]

An analysis of the environmental and personal parameters affecting discomfort in vehicles is provided in the article by Simion *et al.*[12] It was found that thermal sensation in vehicles varies compared to buildings, given that other factors, such as the interior insulation, nonuniform radiant temperature, and solar radiation contribute to the thermal feeling.

Accordingly, the capability of physiological sensors to detect thermal discomfort was explored. For instance, skin conductance and temperature sensors were used as detectors of the body's thermal response. Additionally, different methods have been proposed to detect thermal sensation using thermal imaging.[13] For example, an approach referred to as "Thermal-sense" was proposed using thermal images to detect discomfort using indicators of vasoconstriction and vasodilation.[14]

DATASET

Subjects

Data acquisition was performed using an enclosure in a laboratory at the University of Michigan. The laboratory consisted of an insulating enclosure, four physiological sensors, and a thermal camera. Data were collected from 50 volunteers. The subjects included 18 females and 32 males with different ages and backgrounds, and

had an age range between approximately 18 and 60. The study was advertised and the majority of the subjects included students and staff of the University of Michigan. The study was approved by the IRB of the university.

Devices

The devices included four physiological sensors, such as skin temperature (ST), skin conductance (SC), blood volume pulse (BVP), and respiration rate (RR) sensors. The electrodes of the SC sensor were connected to the third and second fingers of the subjects. The BVP sensor was connected to the index finger and the ST sensor was connected to the small finger. The RR sensor was placed around the thoracic region. A cost-effective FLIR One thermal camera, which can be easily installed in vehicles, without significantly affecting the vehicle's price, was used to record thermal videos of the faces of the subjects during the comfort and discomfort stages in experiments.

Experimental Procedure

An enclosure was built in a lab using insulating material for isolation from the room temperature. An air conditioning and heat pump unit as well as a fan and an electric heater were connected to the enclosure and used to supply cold/hot air. The enclosure contained a seat for the subjects to sit comfortably as well as a fan and a heater to increase the subjects' sensation of cold and hot, respectively. The enclosure also had a slit to allow the connection of the physiological sensors and the recording of the thermal camera.

The participants were given the instruction to follow during the experiments. This was followed by connecting the four physiological sensors to their left hand and chest. The experiments included three phases as follows.

Comfort First, the participants were asked to stay inside the building until their bodies adjusted to the indoor temperature of the building. They were then instructed to sit on the seat in the enclosure. All of the subjects in our experiments reported that they were feeling thermally comfortable and were recorded for 4 min in this stage.

Cold Discomfort During this phase, cold air was blown inside the enclosure using the ac unit and the fan while the subjects were sitting inside until the temperature inside the enclosure stabilized at approximately 61° F. The subjects were then recorded for 4 min with the cold air still blowing.

Hot Discomfort During this phase, the heat pump and heater were used to blow hot air inside the enclosure until the temperature was above 95° F. The participants were then recorded for four additional minutes.

Thermal Sensation Rating The subjects were asked to evaluate their thermal sensation using the PMV ratings, which are used for indoor steady-state conditions. The PMV ratings fall on a scale of −3–3, for cold to hot. In particular, −3 represents cold, −2 represents cool, −1 indicates slightly cool, 0 indicates neutral, +1 represents slightly warm, +2 represents warm, and +3 indicates hot.

The participants were asked to report their sensation following each phase on the PMV scale. These ratings were used as the ground truth for our multimodal learning approach. Note that while the physiological measurements were extracted from all the subjects, the thermal videos were collected from 22 subjects due to an update error in the FLIR One app.

METHODOLOGY

In this section, the process of extracting features from the physiological modality and the thermal videos is described.

Physiological Signals

The physiological features included the four raw physiological signals as well as statistical measurements derived from them. The heart rate, skin temperature, respiration rate, and skin conductance were collected at a sampling rate of 2048 samples/secs. The extracted measurements also included statistical descriptors derived from the raw signals, such as averages, power means, epochs, standard deviation, minimum, maximum, and features extracted from interbeat intervals.

The final set of the physiological feature vectors included 40 heart rate, five skin temperature, seven respiration rate, and five skin conductance measurements, as well as two heart rate variability features derived from the heart

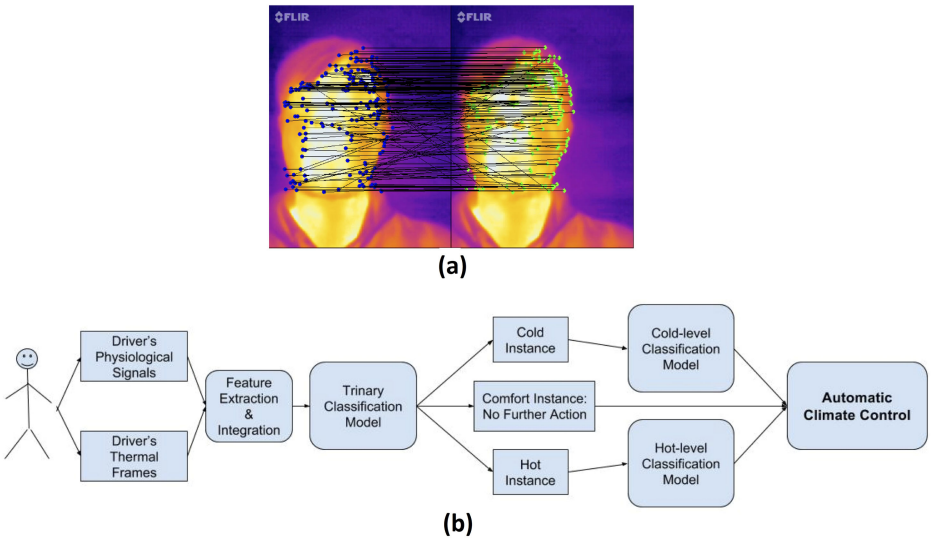

Figure 1. (a) The Detection and tracking processes of interesting points that are usually located where there are sharper changes in temperatures. (b) The proposed cascaded system formed of feature extraction and integration, two-stage classification scheme, and a climate control system.

rate and respiration rate sensors combined. Hence, the final dataset consisted of 59 physiological features.

Thermal Imaging

In order to create feature vectors representing the thermal signatures extracted from the subjects' faces, we underwent three steps including segmentation of the faces, interesting points tracking, and construction of thermal maps. We proposed our tracking approach for thermal images in the article by Abouelenien *et al.*[4] and we build upon our approach.

Segmenting and Tracking Thermal Faces

The thermal faces of the participants were located in the first frame of each thermal video. Interesting points were identified in the faces using the Shi Tomasi detection algorithm, where they were found at pixels with large variation in colors, which represented different temperatures, by calculating the sum of square differences between successive thermal images. In particular, lighter colors indicated higher temperatures that could potentially represent the presence of veins that control the temperature of the skin in the surrounding area.

Following the detection of interesting points, the Kanade Lucas Tomasi tracking method[15] was applied to track these points throughout the subjects' responses, as shown in Figure 1(a). This tracking algorithm works under the assumption of a slight pixel displacement between images, which fits the condition of a driver with limited space to make significant movements in a car. In order to detect outliers and uncertain points, the forward–backward error was computed by tracking the points between frames back and forth. Once the points were tracked from one frame to the next, the bounding boxes surrounding the faces were reconstructed by applying the similarity measures using the global geometric transformation. We set a threshold of 95% matching points between successive frames and five pixels as the maximum allowed distance between tracked points in order to increase the accuracy of the tracking process. Frames that did not meet the threshold were eliminated, and the tracking process proceeded to the next frame.

Thermal Maps Construction Following the segmentation and tracking processes of the thermal faces, a thermal map was constructed from each face by extracting meaningful features that represent the temperature distribution. In order to achieve this target, the face images were binarized and multiplied by the original image in order to isolate the background, assuming that thermal faces consistently have higher temperatures compared to the background. The thermal

faces were then masked and cropped to construct the thermal map.

Thermal maps were constructed by extracting meaningful statistical features that represented the temperature distribution, represented in terms of pixels values, in the thermal faces using the Hue Saturation Value representation. The features include the mean pixel value, maximum pixel value, minimum pixel value, average of the highest 10% pixel values, min–max range, and a histogram of 255 bins of the thermal distribution in the faces in each frame for each of the Hue Saturation Value channels to form a total of 780 features. The histogram features were normalized in order to form a probability distribution of the temperatures and the feature vectors for the frames were averaged to result in a single feature vector representing each thermal video.

Multimodal Learning Approach

In order to evaluate our approach and the effectiveness of the extracted features, we used machine learning using a decision tree classifier. This particular classifier was recommend by previous research for detecting human-related behaviors.[2,16] The evaluation was performed using four different ways. First, our decision tree classifier was trained using the physiological and thermal modalities separately in order to classify test examples as comfort, cold, or hot. The physiological modality used data from all of the 50 subjects (150 instances) and from the 22 subjects (66 instances). This analysis specified the most effective sensors in identifying the thermal sensation of the subjects. Second, instances from both the physiological and thermal modalities from the 22 subjects were integrated using early feature fusion. Third, we went beyond the three-class classification scheme and expanded our approach to detect seven classes by classifying the test vectors into three cold discomfort sensations, three hot discomfort sensations, and one comfort sensation.

Finally, we introduced a cascaded system formed of the two classification stages that include three classification models. This process is realized by first classifying unseen instances into comfort, cold, and hot, and then, introducing the classified instances into two separate cold and hot classification models to determine the different levels of cold discomfort and hot discomfort. This process can be seen in Figure 1(b).

In order to have a reasonable evaluation, leave-one-subject-out cross validation was used with the decision tree classifier by using all three instances of each subject for testing and all other instances for training our system during each fold. This was performed in order to avoid any bias arising from having responses from any subject in both the train and test sets. The performance was evaluated using the average overall classification accuracy and the recall per class, which is calculated as the number of correctly classified instances per class divided by the total number of instances belonging to that particular class. Moreover, the F-measure, which is the weighted harmonic mean of the average recall and average precision of all classes, is used to evaluate the performance. It should be noted that if the true positives and false positives are equal to zero for any specific class, then the precision is determined as zero as well as for that class.

We also compared our results to the baseline performance (listed in each table), which presented the prediction rate for each case using random guessing. This baseline was selected to ensure the system was able to learn useful information from the extracted features and was not performing randomly as compared to the baseline. Moreover, given the novelty of our dataset and our approach that relies solely on data extracted from human responses and the fact that earlier approaches considered, for the most part, environmental factors, such as air temperature, humidity, and air speed without considering the actual human measurements, it was not reasonable to compare to earlier approaches using the PMV model.

EXPERIMENTAL RESULTS

Individual Modalities

Table 1(a) shows the average accuracy and recall for each of the three classes using features from individual and combined sensors. Feature vectors with PMV ratings from -1 to -3 were labeled as the cold class and vectors with ratings from 1 to 3 were labeled as the hot class.

As expected, the table indicates that the skin temperature sensor provides features that are

Table 1. Average accuracy and recall for the four raw physiological signals, feature sets of individual sensors, and all physiological features combined using data from (a) all 50 subjects for each of the cold discomfort, hot discomfort, and comfort classes and (b) 22 subjects in addition to thermal features for each of the cold discomfort, hot discomfort, and comfort classes, and (c) for each of the three cold discomfort, three hot discomfort, and comfort classes.

	Baseline	4-Raw	RR	ST	BVP	SC	All
Accuracy	33.3	74.7	32.0	**76.0**	53.3	39.3	72.0
F-measure		74.4	32.1	**76.0**	53.5	39.3	72.5
Comfort	33.3	60.0	36.0	68.0	52.0	44.0	**72.0**
Cold	33.3	**98.0**	38.0	90.0	60.0	40.0	86.0
Hot	33.3	66.0	22.0	**70.0**	48.0	34.0	58.0

(a)

	Baseline	4-Raw	RR	ST	BVP	SC	All	Thrm
Accuracy	33.3	66.7	34.8	72.7	47.0	37.9	66.7	**74.2**
F-measure		66.9	35.1	73.0	46.9	37.7	66.8	**74.8**
Comfort	33.3	50.0	36.4	63.6	31.8	40.9	45.5	**77.3**
Cold	33.3	**86.4**	31.8	**86.4**	59.1	27.3	**86.4**	68.2
Hot	33.3	63.6	36.4	68.2	50.0	45.5	68.2	**77.3**

(b)

	No.	Baseline	4-Raw	RR	ST	BVP	SC	All	Thrm
Accuracy		33.3	**54.5**	25.8	39.4	21.2	25.8	42.4	45.5
F-measure			**39.1**	17.9	24.2	18.3	14.1	32.7	38.3
Comfort	22	33.3	**86.4**	40.9	77.3	22.7	54.5	68.2	63.6
Cold -1	6	9.1	0	0	0	0	0	**16.7**	**16.7**
Cold -2	9	13.6	**66.7**	33.3	33.3	55.6	22.2	44.4	33.3
Cold -3	7	10.6	28.6	14.3	28.6	28.6	0	**42.9**	0
Hot 1	7	10.6	42.9	14.3	0	0	0	14.3	**85.7**
Hot 2	11	16.7	**54.5**	27.3	36.4	18.2	27.3	36.4	**54.5**
Hot 3	4	6.1	0	0	0	0	0	0	0

(c)

capable of determining the thermal discomfort levels of the participants. The features from the BVP sensor achieve the second-best performance, while the respiration rate and skin conductance sensors provide a poor performance. The table also shows that the cold class is the best detectable sensation for the subjects reaching a recall of 98% using all four raw features.

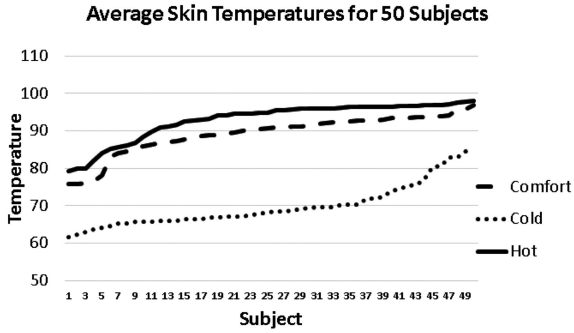

Figure 2. Sorted cold, hot, and comfortable average temperatures for all 50 subjects.

To further evaluate the improved performance of the cold class over other classes and analyze the reasons the skin temperature features stand out, Figure 2 shows the sorted average temperatures from the skin temperature sensor for all 50 subjects for the cold, hot, and comfort classes.

Three interesting observations can be noticed in the figure. First, the cold curve is well isolated from the other curves, whereas the hot and comfort curves fall in a closer range. Second, as seen by the sorted temperatures, some ranges represent a comfortable sensation to some subjects, whereas at the same time representing hot sensation for others. This indicates that the thermal sensation for human is highly subjective. Finally, the time duration needed to reach a certain level of cold discomfort from the comfort sensation is approximately double that is needed to transfer from the cold sensation to the hot sensation, which indicates that human bodies have faster adaptation to heat.

Table 1(b) lists similar results to Table 1(a) using the data collected only from the 22 subjects that had thermal video recordings. The last column in the table also lists the overall accuracy and recall using the thermal features for comparison. For the physiological features, the same trends can be observed as earlier, where the skin temperature features, followed by the raw features, and all physiological features combined exhibit the best performance. However, by cross-referencing Table 1(a), it can be noticed that there is a slight drop in accuracy in the majority of cases, which can be a result of having a lower number of training instances in each fold using 22 subjects. The thermal features evidently exhibit improved performance compared to the physiological sensors, especially for the average accuracy and recall of the comfort and hot classes. The F-measure results agree with the accuracy as well for both tables.

We extend the classification system to classify seven different classes of comfort and discomfort sensations. Table 1(c) lists the average accuracy and recall of the three cold discomfort, three hot discomfort, and comfort classes for the raw data, feature sets from individual physiological sensors, all physiological features combined, and the thermal features. The second column shows the number of vectors that belong to each class.

The table indicates that the four raw physiological measurements achieve the highest accuracy as well as the best recall in most cases followed by the thermal features. The performance of the raw features, skin temperature features, all physiological features combined, and the thermal features is generally above the baseline. The poorest performance is once again achieved by the heart and respiration rate sensors. The F-measure follows the same trend as the accuracy while showing a drop in performance as it is measured using the average recall and precision of all the seven classes. Clearly, the learning process fails for Cold −1 and Hot 3 classes due to training with insufficient number of instances. In general, the process can differentiate between different classes; however, it is expected to improve with the availability of more instances.

Bimodal Classification Into Three Classes

As it was observed earlier that the thermal features and the skin temperature sensor achieve improved performance, we explore the effectiveness of integrating these features together in the learning process.

Table 2(a) lists the overall accuracy and recall of the three classes for the integration of the thermal features with individual and combined physiological features. The table indicates that the fusion of the thermal features, especially with the skin temperature features, exhibits superior performance compared to all other fusions as well as to their individual performances, as seen earlier in Table 1(b). It can also be noted that the fusion of the thermal features with the four raw features and all physiological features combined achieves identical performance, which indicates that the learning process only utilized the thermal and skin temperatures' features through different folds to create the classification model. The confusion matrix for the "Thrm + All" is given in Table 2(b), which is also reflected in the improved recall of all three classes.

Bimodal Classification Into Seven Classes

The fusion of the thermal features with the individual and combined physiological features is extended to classify unseen instances into the seven classes in Table 2(c). While the best accuracy does not exceed that of the four raw features in Table 1(c), there is a general improvement in the accuracy and recall figures. For instance, the Cold −1 class exhibits improved performance with the combination of the thermal features with different physiological features.

Cascaded System

In order to develop a more reliable and effective approach to detect human thermal discomfort, we propose a cascade of decision tree classifiers designed to learn separately different degree of hot and cold thermal discomfort as well to avoid the uncertainty associated with learning from a large number of classes at once. The proposed cascaded system includes three separate classification models within a two-stage classification framework.

The first stage represents a trinary classification model that aims at classifying the human

Table 2. Average accuracy and recall for the fusion of the thermal features with the physiological raw signals, feature sets from individual sensors, and all physiological features combined for (a) each of the cold discomfort, hot discomfort, and comfort classes and (c) each of the three cold discomfort, three hot discomfort, and comfort classes. The confusion matrices for the "Thrm+All" 3-class classification and the "Thrm+All" 7-class classification are shown in (b) and (d), respectively.

	Baseline	Thrm +4Raw	Thrm +RR	Thrm +ST	Thrm +BVP	Thrm +SC	Thrm +All
Accuracy	33.3	**87.9**	74.2	**87.9**	74.2	74.2	**87.9**
F-measure		**88.1**	74.8	**88.1**	74.8	74.8	**88.1**
Comfort	33.3	**86.4**	77.3	**86.4**	77.3	77.3	**86.4**
Cold	33.3	**86.4**	68.2	**86.4**	68.2	68.2	**86.4**
Hot	33.3	**90.9**	77.3	**90.9**	77.3	77.3	**90.9**

(a)

	Comf	Cold	Hot
Comf	**19**	0	3
Cold	2	**19**	1
Hot	1	1	**20**

(b)

	No.	Baseline	Thrm +4Raw	Thrm +RR	Thrm +ST	Thrm +BVP	Thrm +SC	Thrm +All
Accuracy		33.3	48.5	45.5	48.5	45.5	45.5	**51.5**
F-measure			35.8	37.6	35.8	37.9	37.9	**40.1**
Comfort	22	33.3	**81.8**	63.6	**81.8**	63.6	63.6	**81.8**
Cold -1	6	9.1	0	16.7	0	**33.3**	16.7	**33.3**
Cold -2	9	13.6	**33.3**	**33.3**	**33.3**	22.2	**33.3**	22.2
Cold -3	7	10.6	0	0	0	0	0	**14.3**
Hot 1	7	10.6	**85.7**	**85.7**	**85.7**	**85.7**	**85.7**	**85.7**
Hot 2	11	16.7	45.5	**54.5**	45.5	**54.5**	**54.5**	45.5
Hot 3	4	6.1	0	0	0	0	0	0

(c)

	Comf	Cold-1	Cold-2	Cold-3	Hot 1	Hot 2	Hot 3
Comf	**18**	3	0	0	0	1	0
Cold-1	0	**2**	1	1	1	1	0
Cold-2	0	1	**2**	6	0	0	0
Cold-3	1	3	2	**1**	0	0	0
Hot 1	0	1	0	0	**6**	0	0
Hot 2	0	2	0	0	4	**5**	0
Hot 3	0	2	0	0	2	0	**0**

(d)

instances into three classes of neutral, cold, and hot discomfort using our cross-validation technique described earlier. The second stage elaborates the detection process by further classifying the detected hot and cold groups into different levels of hot as well as different levels of cold discomfort using two parallel classification models. In this case the training process is performed separately using only the instances detected as hot from the first stage and using only the instances detected as cold for the hot-level classification model and the cold-level classification model, respectively. The accuracy and recall results in Table 3(a) reflect the accuracy of the input to the

Table 3. Average accuracy and recall of each of the three cold discomfort, three hot discomfort, and comfort classes for the fusion of the thermal features with the physiological raw signals, feature sets from individual sensors, and all physiological features combined using (a) the cascaded system. The confusion matrix for the "Thrm + All" for the cascaded system is shown in (b).

	No.	Baseline	Thrm +4Raw	Thrm +RR	Thrm +ST	Thrm +BVP	Thrm +SC	Thrm +All
Accuracy		33.3	48.5	48.5	48.5	**51.5**	48.5	**51.5**
F-measure			38.7	38.7	38.7	**43.6**	38.7	**43.6**
Comfort	22	33.3	**86.4**	**86.4**	**86.4**	**86.4**	**86.4**	**86.4**
Cold -1	6	9.1	0	0	0	**33.3**	0	**33.3**
Cold -2	9	13.6	11.1	11.1	11.1	**22.2**	11.1	**22.2**
Cold -3	7	10.6	0	0	0	**14.3**	0	**14.3**
Hot 1	7	10.6	**71.4**	**71.4**	**71.4**	57.1	**71.4**	57.1
Hot 2	11	16.7	**45.5**	**45.5**	**45.5**	36.4	**45.5**	36.4
Hot 3	4	6.1	**50**	**50**	**50**	**50**	**50**	**50**

(a)

	Comf	Cold-1	Cold-2	Cold-3	Hot 1	Hot 2	Hot 3
Comf	**19**	0	3	0	0	0	0
Cold-1	1	**2**	0	2	1	0	0
Cold-2	0	3	**2**	4	0	0	0
Cold-3	1	0	5	**1**	0	0	0
Hot 1	0	1	0	0	**4**	0	2
Hot 2	1	0	0	0	5	**4**	1
Hot 3	0	0	0	0	1	1	**2**

(b)

"Automatic Climate Control" block in Figure 1(b). It should be noted that if an instance is misclassified using the trinary classification model in the figure, then it will be also misclassified during the second stage classification.

The table provides interesting observations. First, although the best overall accuracy is similar to that in Table 2(c), having separate classification models enriches the learning process, which is reflected in the improvement of the accuracy and recall figures in most cases. For example, the Hot 3 class achieves 50% recall compared to a consistent misclassification pattern in all previous cases. This is also reflected by comparing the confusion matrices of "Thrm+All" in Table 3(b) and Table 2(d). Second, interestingly the performance of the fusion of the thermal features with the heart rate features exceeds that of their fusion with the skin temperature features. This can be explained with the high recall for the comfort class that the thermal and skin temperature features were achieving in Table 2(c), which improved the overall accuracy. In that table, however, the performance of the other sensors was comparable and sometimes better for classes other than the comfort class. For the cascaded system in Table 3(a), the performance of the comfort class is balanced among the different sets of features and, hence, other fusions achieve improved performance.

CONCLUSION

In this article, we introduced a novel learning approach representing the progress of developing a fully automated climate control system in vehicles, which included a novel

dataset and an extensive analysis of physiological and thermal features in order to detect human discomfort.

Our results showed that the thermal features as well as specific physiological signals, such as the skin temperature and all physiological features combined were capable of indicating the thermal discomfort state of the subjects as well as different levels of hot and cold discomfort. Evidently, the integration of the thermal features with other physiological features enhanced the performance significantly with a relative improvement of 18.5% over the best accuracy achieved by any single feature set. The introduced cascaded system enriched the learning process and increased the reliability of the climate control system by learning separate models for the hot and cold discomfort. Furthermore, the separate models shed some light on the usefulness of other physiological features, such as the heart rate when learning from a smaller number of instances. It is expected that the effectiveness and reliability of the system will increase as more data is collected. Our analysis indicated the feasibility of implementing automated thermal sensation detection systems in vehicles.

REFERENCES

1. D. Williams, "The Arbitron national in-car study." Arbitron Inc., New York, NY, USA, Tech. Rep., 2009.
2. M. Abouelenien, V. Prez-Rosas, R. Mihalcea, and M. Burzo, "Detecting deceptive behavior via integration of discriminative features from multiple modalities," *IEEE Trans. Inf. Forensics Secur.*, vol. 12, no. 5, pp. 1042–1055, May 2017, doi:10.1109/TIFS.2016.2639344.
3. M. Abouelenien *et al.*, "Gender differences in multimodal contact-free deception detection," *IEEE MultiMedia*, vol. 26, no. 3, pp. 19–30, Jul.–Sep. 2019, doi:10.1109/MMUL.2018.2883128.
4. M. Abouelenien *et al.*, "Detecting human thermal discomfort via physiological signals," in *Proc. 10th Int. Conf. Pervasive Technol. Related Assistive Environ.*, 2017, pp. 146–149, doi:10.1145/3056540.3064957, http://doi.acm.org/10.1145/3056540.3064957
5. M. Cornacchia, K. Ozcan, Y. Zheng, and S. Velipasalar, "A survey on activity detection and classification using wearable sensors," *IEEE Sensors J.*, vol. 17, no. 2, pp. 386–403, Jan. 2017, doi:10.1109/JSEN.2016.2628346.
6. M. Abdallah *et al.*, "Sensing occupant comfort using wearable technologies," in *Proc. Construction Res. Congr.*, 2016, pp. 940–950.
7. C. Urmson and W. Whittaker, "Self-driving cars and the urban challenge," *IEEE Intell. Syst.*, vol. 23, no. 2, pp. 66–68, Mar. 2008, doi:10.1109/MIS.2008.34.
8. L. Li, J. Song, F.-Y. Wang, W. Niehsen, and N.-N. Zheng, "IVS 05: New developments and research trends for intelligent vehicles," *IEEE Intell. Syst.*, vol. 20, no. 4, pp. 10–14, Jul./Aug. 2005, doi:10.1109/MIS.2005.73.
9. N.-N. Zheng, S. Tang, H. Cheng, Q. Li, G. Lai, and F.- Wang, "Toward intelligent driver-assistance and safety warning system," *IEEE Intell. Syst.*, vol. 19, no. 2, pp. 8–11, Mar./Apr. 2004, doi:10.1109/MIS.2004.1274904.
10. Y. Lin *et al.*, "Study on human physiological adaptation of thermal comfort under building environment," *Proc. Eng.*, vol. 121, pp. 1780–1787, 2015, doi: http://dx.doi.org/10.1016/j.proeng.2015.09.157, http://www.sciencedirect.com/science/article/pii/S1877705815029859
11. R. Z. Homod *et al.*, "{RLF} and {TS} fuzzy model identification of indoor thermal comfort based on PMV/PPD," *Building Environ.*, vol. 49, pp. 141–153, 2012.
12. M. Simion, L. Socaciu, and P. Unguresan, "Factors which influence the thermal comfort inside of vehicles," *Energy Proc.*, vol. 85, pp. 472–480, 2016, doi: http://dx.doi.org/10.1016/j.egypro.2015.12.229, http://www.sciencedirect.com/science/article/pii/S1876610215028945
13. M. Burzo *et al.*, "Thermal discomfort detection using thermal imaging," in *Proc. ASME Int. Mech. Eng. Congr. Expo.*, 2017, Art. no. V006T08A048.
14. J. Ranjan and J. Scott, "ThermalSense: Determining dynamic thermal comfort preferences using thermographic imaging," in *Proc. ACM Int. Joint Conf. Pervasive Ubiquitous Comput.*, Sep. 2016, pp. 1212–1222.
15. S. N. Sinha *et al.*, "GPU-based video feature tracking and matching," The University of North Carolina at Chapel Hill, Chapel Hill, NC, USA, Tech. Rep., vol. 278, p. 4321, 2006.
16. T. Meservy *et al.*, "Deception detection through automatic, unobtrusive analysis of nonverbal behavior," *IEEE Intell. Syst.*, vol. 20, no. 5, pp. 36–43, Sep./Oct. 2005.

Mohamed Abouelenien is an Assistant Professor with the Department of Computer and Information Science, University of Michigan-Dearborn. He was a Postdoctoral Research Fellow in the Electrical Engineering and Computer Science Department, University of Michigan, Ann Arbor from 2014 to 2017. In 2013, he received the Ph.D. degree in Computer Science and Engineering from the University of North Texas. His research interests include multimodal deception detection, multimodal sensing of thermal discomfort and drivers' alertness levels, emotion and stress analysis, machine learning, ensemble learning, image processing, face and action recognition, and natural language processing. He is the corresponding author of this article. Contact him at: zmohamed@umich.edu.

Mihai Burzo is an Assistant Professor of Mechanical Engineering with the University of Michigan-Flint. Prior to joining University of Michigan, in 2013, he was an Assistant Professor with the University of North Texas. His research interests include heat transfer in microelectronics and nanostructures, thermal properties of thin films of new and existing materials, multimodal sensing of human behavior, and computational modeling of forced and natural heat convection. He is the recipient of several awards, including the 2006 Harvey Rosten Award For Excellence for "outstanding work in the field of thermal analysis of electronic equipment." Contact him at: mburzo@umich.edu.